Beilstein-Institut
Beilstein Bozen Symposium on Molecular Engineering and Control
May 14th – 18th, 2012, Prien (Chiemsee), Germany

Nanoparticle Superlattice Engineering with DNA

Robert J. Macfarlane* and Chad A. Mirkin

Department of Chemistry, Northwestern University, 2145 Sheridan Rd., Evanston, IL 60208, U.S.A.

E-Mail: *rmacfarl@u.northwestern.edu

Received: 30th January 2013 / Published: 13th December 2013

A major challenge in materials synthesis is developing methodologies to synthesize materials by design, the concept that one can know what building blocks are necessary to create a material *a priori* to synthesis. Typically, the building blocks used to synthesize these materials are atoms or molecules, and the identity of the structure being assembled is a function of which atoms are used and how those atoms are bonded to one another. However, developing materials by design using atoms as building blocks is a significant challenge, as the complex factors that dictate how atoms interact with one another makes predicting what structure will be created from a given set of building blocks a difficult task. Moreover, programmability of these interactions is impossible due to the fact that certain factors (such as electronegativity or atomic number) are immutable for atoms. Therefore, once a given set of atoms is chosen, the resulting structures that can be created are inherently linked to the set of building blocks being used. Linus Pauling famously developed a set of rules that explain (in the context of ionic solids) why certain lattices are preferred over others [1]. However, these rules are really a look backwards, as they lack true predictive power and do not always apply to all ionic solids. Given the challenges associated with using atomic or molecular species as building blocks to create materials by design, a more amenable strategy would be to choose building blocks that are more controllable.

In principle, nanoparticles should offer a much better alternative for synthesizing designer materials, due to the large number of factors that can be manipulated in each building block. For example, one can synthesize different sets of nanoparticles that are identical in terms of their elemental composition, but vary in size or shape [2 – 8]; alternatively, one can synthesize two nanoparticles that are structurally identical at the nanometer scale, but are composed of different atomic constituents [4, 9 – 16]. This versatility provides significantly greater

programmability in building block design, and, subsequently, in materials synthesis. However, the challenge associated with using nanoparticles as building blocks is that nanoparticles do not inherently have components that allow them to bond to one another in the manner that electrons allow for atomic bonds to be created. Therefore, to assemble nanoparticles into hierarchical structures, ligands must be attached to the surface of the nanoparticles to dictate how nanoparticles interact with each other [17 – 22]. Many different ligands have been utilized to achieve this, taking control of ionic [20], van der Waals [21 – 22], or biological recognition interactions [17, 18] to dictate nanoparticle bonding patterns. An ideal ligand choice to achieve these types of interactions is DNA. DNA is a linear polymer consisting of a series of nucleobases, where the length of the DNA strand is dictated by the number of nucleobases, and interactions between different DNA strands are dictated by the sequence of those bases – two DNA strands will only hybridize to one another if they contain complementary base sequences. DNA is readily synthesized via automated procedures, and can be readily modified with many different functional groups, enabling its attachment to a wide variety of nanoparticle compositions [23 – 27].

In 1996, the Mirkin group developed the concept of the polyvalent-DNA nanoparticle conjugate, now referred to as the spherical nucleic acid nanoparticle conjugate (SNA-NP). This structure consists of a nanoparticle core, functionalized with a dense monolayer of synthetic oligonucleotides. SNA-NPs have been synthesized with a range of different nanoparticle core compositions, including noble metals (Au [18], Ag [25]), semiconductors (CdSe [28]), oxides (SiO_2 [27], Fe_3O_4 [23]), and polymeric materials [29]. They possess both properties associated with their inorganic core, such as plasmon resonances in the case of noble metals, and the programmable recognition capabilities of DNA. Importantly, they also possess emergent properties that are a direct result of attaching a dense layer of DNA strands to the surface of a nano-object, including enhanced binding strengths [30], innate cellular uptake [31], and greater discrimination against nucleobase sequence mismatch [32]. These enhanced properties have enabled their use in multiple applications, including low limit of detection diagnostics [33] and gene regulation [34].

Since the development of the SNA-NP conjugate in 1996, the Mirkin group, along with others, have taken major strides in being able to utilize this structure as a building block in the synthesis of ordered arrays of nanoparticles. Although early attempts yielded materials that exhibited no long range ordering, short-range ordering and interparticle distance control was demonstrated in subsequent years [35]. Long-range ordering and crystalline materials were achieved for the first time in 2008 by altering the SNA-NP design to utilize DNA linker strands to connect the nanoparticles [36]. These linkers consisted of three basic regions: a recognition sequence complementary to the DNA sequence physically attached to the nanoparticle, a spacer sequence used to control the length of the DNA linker, and a short sticky end presented at the hydrodynamic radius of the SNA-NP. Hybridization interactions between sticky ends on adjacent SNA-NPs allow the nanoparticle to link to one

another. Because each SNA-NP can be attached to tens to hundreds of DNA linker strands (depending on the nanoparticle core size) [24], each nanoparticle can form tens to hundreds of DNA connections to adjacent particles.

It is therefore the key hypothesis of our efforts in SNA-NP assembly that, because the driving force for crystallization is the formation of duplex DNA linkages:

The most stable structure will maximize the number of duplex DNA connections between particles.

The simplicity of this hypothesis allows us to understand the behavior of the SNA-NPs in the context of assembly so well that we have been able to develop a set of design rules for the process of crystal formation [17]. Like Pauling's rules for atoms, these rules explain the relative stability of different lattices as a function of their DNA and nanoparticle building blocks. However, unlike Pauling's rules, this rule set allows one to predict the stability of crystal structures before they are ever synthesized. Therefore, one can direct the formation of a desired crystal structure by controlling different aspects of the building blocks, such as nanoparticle size, nanoparticle shape, DNA length, or DNA sequence [17].

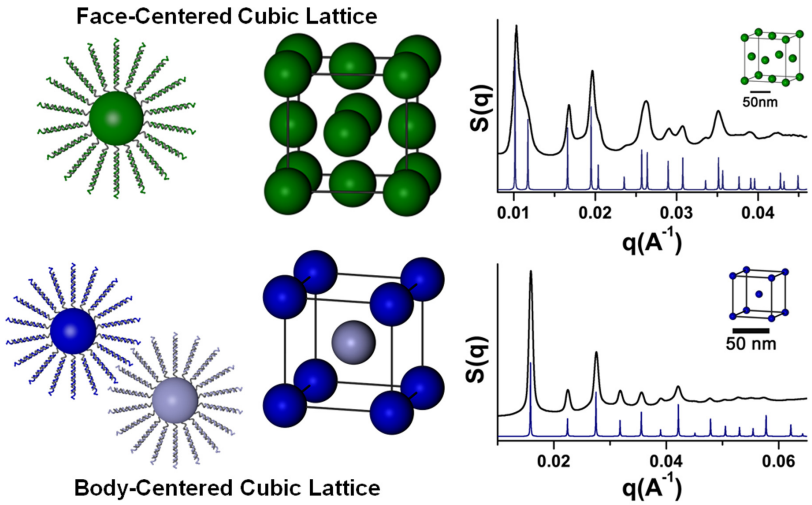

Figure 1. Face-centered cubic lattices are obtained from DNA with self-complementary sticky end sequences, and body-centered cubic lattices are obtained in a binary system where two NPs are functionalized with DNA that contain complementary sticky ends; all lattices are confirmed via small angle X-ray scattering. Figure adapted from ref. 17 (reprinted with permission from publisher).

The first rule in DNA-mediated assembly is: SNA-NPs of equal hydrodynamic radii will form an fcc lattice when using self-complementary DNA sequences, and a bcc lattice when using two SNA-NPs with complementary DNA sequences (Fig. 1). When assembling

particles with a self-complementary sticky end, all particles are able to form DNA linkages with all other particles in solution. Therefore, the maximum number of DNA duplexes are formed when each particle is surrounded by the largest number of nearest neighbors, which is achieved when the particles are arranged in a face-centered cubic lattice. This is because fcc lattices represent the densest packing of spheres of a single size. However, when two different sets of particles are combined with sticky ends that are complementary to each other, the maximum number of DNA duplexes is achieved with a body centered cubic arrangement. This is due to the fact that, while a bcc arrangement does not maximize the total number of nearest neighbors for each particle, it does maximize the number of complementary nearest neighbors – the number of nearest neighbors to which a particle can actually form a connection.

To achieve these lattices, particles are combined with the appropriate DNA linkers, then allowed to aggregate. The aggregate (which is initially a disordered, kinetic structure) is annealed, and the thermal energy allows the particles to reposition themselves within the lattice to form an ordered structure. The identity of the lattice is confirmed using small angle X-ray scattering (SAXS), as well as transmission electron microscopy (TEM) (Fig. 2).

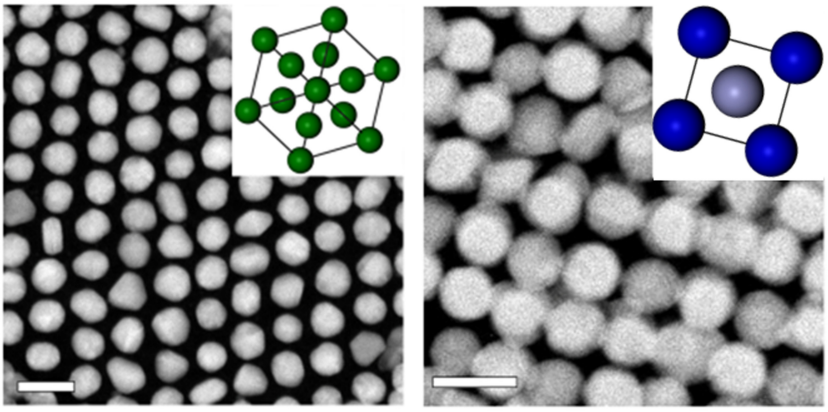

Figure 2. TEM images of fcc (left) and bcc (right) lattices, along with models showing the corresponding lattice orientation (insets). Scale bars are 50 nm. Figure adapted from ref. 17 (reprinted with permission from publisher).

An important aspect of this rule is that it applies to many different particle sizes and DNA lengths. Nanoparticles between 5 and 80 nm have been crystallized into fcc and bcc lattices, where the lattice parameters were controlled to be between 25 and 225 nm [17, 37 – 38]. Importantly, because the nanoparticle size and DNA length are each independent variables, either one (or both) can be used to control the lattice parameters and interparticle distances within a lattice. Thus, nanoparticles can be assembled in a lattice where the unit cell edge length is not dictated by the size of the particles being assembled.

In addition to the large amount of programmability afforded in dictating lattice parameters, this DNA-mediated assembly process also enables a high degree of precision in particle placement. By examining the interparticle distance for each of the fcc and bcc lattices synthesized, the DNA linker rise per base pair (bp) value can be calculated. This value is the increase in interparticle distance afforded by making a DNA strand one basepair (bp) longer, and is calculated to be ~0.255 nm/bp for all fcc and bcc lattices synthesized. This indicates that the DNA-mediated assembly process affords nanometer-scale precision in dictating the lattice parameters of a crystal, as each additional base in a DNA linker adds less than one nanometer to the interparticle distance in the crystal.

In addition to controlling the length of the DNA linkages between particles, it is also possible to control the strength of an individual DNA sticky end duplex, which allows for kinetic products to be accessed. A corollary to the first design rule is therefore that, for two lattices of similar stability, kinetic products can be produced by slowing the rate at which individual DNA linkers de- and subsequently re-hybridize. In order for a lattice to transition from an initial kinetic product to the thermodynamically most favorable state, DNA linkages that tether a nanoparticle in place must be broken, thereby allowing the nanoparticle to reposition itself within an aggregate, where new DNA connections can be formed [39]. Each DNA de- and subsequent re-hybridization event occurs on the timescale of microseconds; this is due to the weak nature of individual sticky end duplexes (which allows DNA duplexes to be rapidly broken) and the high local concentration of DNA (which allows the DNA strands, once separated, to find and hybridize to another adjacent DNA sticky end). By using temperature to control the rate at which these hybridization and dehybridization events occur, one can lock in kinetic products that exist as metastable states. For example, a hexagonal close-packed (hcp) arrangement positions individual nanoparticles to have the same number of nearest neighbors as a particle in an fcc lattice (Fig. 3).

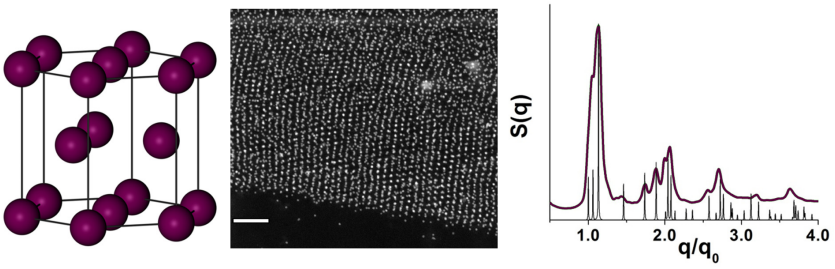

Figure 3. HCP lattices can be obtained as kinetic products by controlling the reorganization rate of particles within a lattice. Scale bar is 100 nm. Figure adapted from ref. 17 (reprinted with permission from publisher).

HCP lattices are only observed as kinetic products in these systems, due to a slight favorability in the energetics of fcc lattices [36, 40]. However, hcp lattices can be observed as kinetic products at early time points in the formation of fcc lattices, as their simpler packing

structure enables them to be more readily observed in small clusters of particles. These hcp lattices can be stabilized by slowing the rate of reorganization (i. e., slowing the rate at which DNA bonds are formed and/or broken during the crystallization process). This promotes the growth of hcp clusters over their reorganization to the more favored fcc lattice. This highlights the high degree of control afforded by using DNA strands to assemble nanoparticles.

The distance between two nanoparticles in lattices that are linked with DNA is determined as the sum of the inorganic nanoparticle radii and the length of the DNA linker strands. However, two SNA-NPs that are bound together only interact at their hydrodynamic radius, meaning that there is no direct interaction between the inorganic cores. This allows one to separately control the radius of an inorganic nanoparticle and the overall hydrodynamic radius of an SNA-NP.

Therefore, the second rule of DNA-programmed nanoparticle assembly is:

The overall hydrodynamic radius of a SNA-NP, rather than the sizes of its individual NP or oligonucleotide components, dictates its assembly and packing behavior.

In other words, two nanoparticles can be made to behave as if they were exactly the same size, even if they possess inorganic nanoparticle cores of widely different diameters; this is achieved by altering the DNA linker lengths on the two particles so that the sums of the DNA length and nanoparticle core are equivalent (Fig. 4). This enables the synthesis of CsCl-type lattices, which exhibit the same connectivity as bcc lattices, but utilize particles of with different inorganic cores. Interestingly, appropriate choice of DNA linker lengths allows for two particles to have the same hydrodynamic radius (and therefore same assembly behavior) even if one particle has an inorganic core that is three times the size of the other.

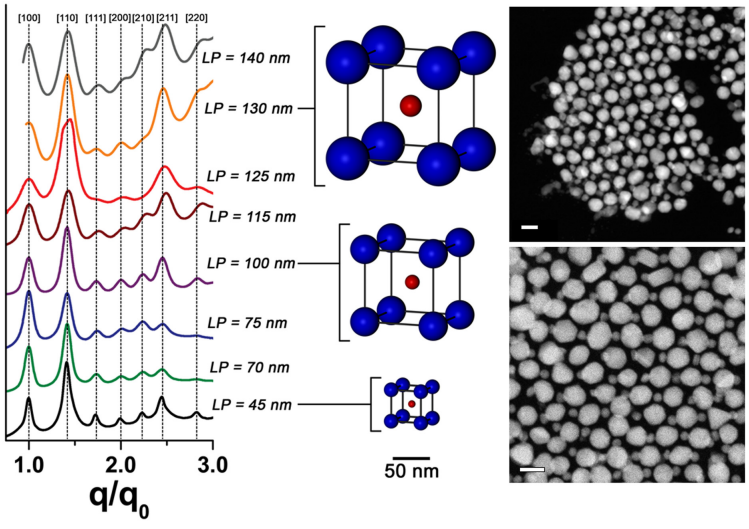

Figure 4. The hydrodynamic radius of a particle dictates its assembly parameters; this can be used to generate CsCl-type lattices. Scale bars are 100 nm. Figure adapted from ref. 17 (reprinted with permission from publisher).

The third rule for DNA-programmed assembly is:

In a binary system based upon complementary SNA-NPs, favored products will tend to have equivalent numbers of each complementary DNA sequence, evenly spaced throughout a unit cell.

In order to achieve more complex crystallographic symmetries, DNA and nanoparticle combinations must be used where, unlike the fcc, bcc, and CsCl lattices mentioned previously, nanoparticle assembly behavior is not equivalent for the two particles in a binary system. This is most readily achieved by changing the ratio of the hydrodynamic sizes of the particles, or by changing the relative number of DNA strands on each particle. The size ratio affects the packing of the SNA-NPs by controlling where particles are positioned relative to one another. For example, a particle with a large hydrodynamic radius can be surrounded by a large number of particles with a relatively small hydrodynamic radius, but each small particle can only be surrounding by a few larger particles; one would therefore predict that the most favored unit cell for this pairing would have a particle stoichiometry that favors the presence of a larger number of the smaller particles. The ratio of the number of DNA strands on each particle type has a different, but equally important effect. Because the driving force for crystallization is the maximization of the number of DNA linkages formed, it is reasonable to assume that a favored unit cell will have roughly equivalent numbers of DNA linkers of complementary types. In other words, if, in a binary system, one particle has twice the number of DNA linkers attached to it, the most favored unit cell will most likely have half as many of that type of particle, so that there are equal numbers of DNA linkers of opposite types. By manipulating these two variables (hydrodynamic size ratio and linker number ratio), three additional crystal structures can be synthesized, isostructural with AlB_2, Cr_3Si, and the alkali-fullerene complex Cs_6C_{60} (Fig. 5). Each of these lattice can be synthesized with varied lattice parameters and particle sizes, in the same manner as the fcc, bcc, and CsCl structures.

Interestingly, when comparing the binary lattices synthesized with this method, a trend can be observed that given crystal symmetries tend to favor specific values of hydrodynamic size ratio and/or DNA linker number ratio.

Thus, rule four is:

Two systems with the same size ratio and DNA linker ratio exhibit the same thermodynamic product.

The importance of this rule is that, once a crystal structure has been synthesized, it allows one to ‘‘dial in’’ a crystal structure using different particle sizes or DNA lengths, simply by tailoring the size and linker ratios to match those of the initial crystal structure. Perhaps more important is the implication that, if these two variables can be used to determine which

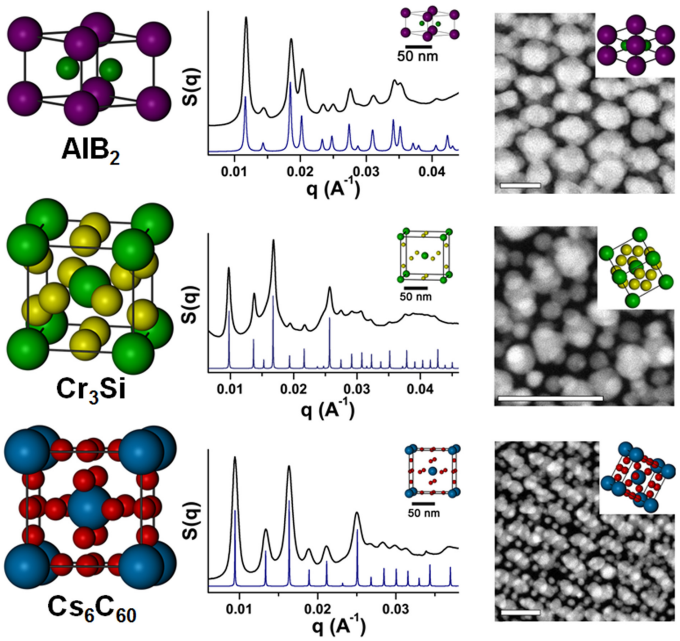

Figure 5. Controlling particle size ratio and DNA linker ratio in a binary system enable the synthesis of lattices with different particle stoichiometries. Scale bars are 50 nm. Figure adapted from ref. 17 (reprinted with permission from publisher).

crystal structure is most stable, one should be able to develop a phase diagram with these two variables as axes. Although it is not possible to directly measure the number of DNA duplexes formed in a given structure (nor to measure the number of DNA duplexes in an unstable structure that does not form), it is possible to develop computational methods that predict these values as a function of nanoparticle size, DNA length, and crystal symmetry. To achieve this, a mean-field model was developed based on established properties of both DNA (such as rise per base pair and persistence length [38]) and SNA-NPs (such as the number of DNA strands per particle [24]). This model was then used to calculate the number of DNA duplexes formed as a function of size ratio, linker ratio, and crystal symmetry, and to construct a phase diagram that predicted which crystal symmetry maximized DNA hybridization interactions for a given size and linker ratio combination (Fig. 6).

It is important to note that many different crystal symmetries were examined, and, for each region of the phase diagram, the most stable symmetry was always found to be one of the four crystal structures obtained experimentally. Moreover, a comparison of the modeled phase diagram and the experimental data demonstrated greater than 90% agreement between the two; i.e. over 90% of the crystal structures obtained experimentally were correctly predicted by the phase diagram as being the most stable arrangement of particles.

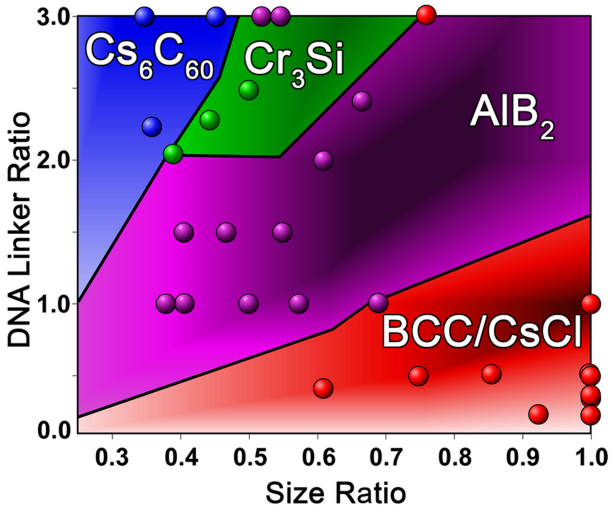

Figure 6. Phase diagram relating experimentally controllable parameters to predicted crystal structure. Experimental data points are shown to correlate with theoretical phase diagram and are color coded to the experimentally observed structure. Figure adapted from ref. 17 (reprinted with permission from publisher).

Because each of the SNA-NPs used to assemble these superlattices is functionalized with a large number of DNA strands, it is possible to put multiple DNA sequences on a single nanoparticle.

Therefore, the fifth rule of DNA-programmed assembly is:

SNA-NPs can be functionalized with more than one oligonucleotide bonding element, providing access to crystal structures not possible with single element SNA-NPs.

For example, a SNA-NP that is functionalized with linkers containing self-complementary sticky ends would be predicted to form an fcc lattice as its thermodynamic product, as per rule 1. However, if this SNA-NP were also functionalized with a second type of DNA linker that contained a sticky end complementary to the sticky ends of a different SNA-NP, additional DNA linkages could be created. This enables the synthesis of NaCl-type lattices, where the self-complementary sticky ends dictate the formation of an fcc lattice, but the additional sticky ends allow a second nanoparticle to fill into the octahedral holes in the fcc lattice while it forms (Fig. 7).

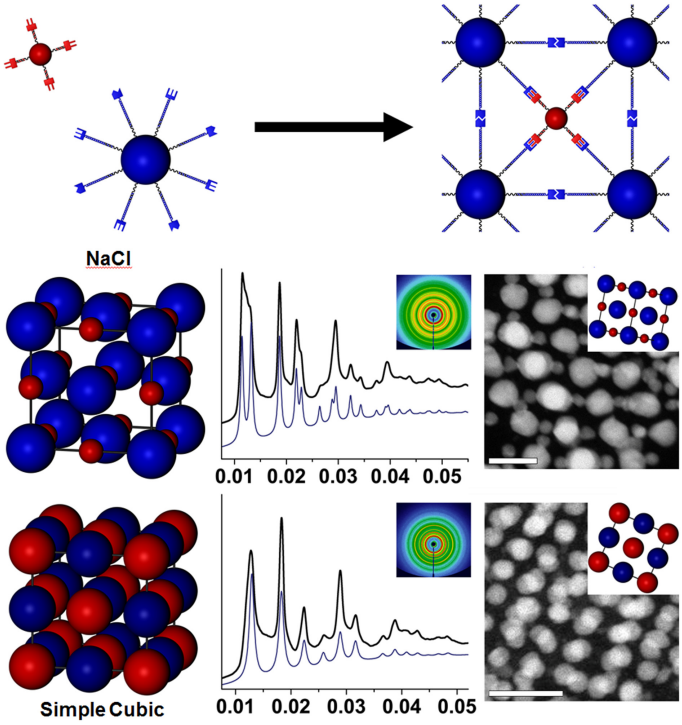

Figure 7. By hybridizing multiple types of linkers to a single SNA-NP, multiple types of DNA bonds can be generated in a single lattice. Scale bars are 50nm. Figure adapted from ref. 17 (reprinted with permission from publisher).

It should be noted, however, that the hydrodynamic size ratio of the two particles must be ~0.40 in order to form an NaCl lattice. If one of the particles has a hydrodynamic radius that is too large or too small, the sticky ends will not be positioned at the correct location to enable both the self- and non-self-complementary linkages to be formed at the same time. However, as mentioned in the second rule, the inorganic nanoparticle core size can be varied separately from the hydrodynamic radius. When assembling a NaCl-type lattice where the hydrodynamic size ratio is still ~0.40, but the inorganic particle core sizes are equal, it is actually a simple cubic lattice that is formed (as defined by the positions of the inorganic cores) (Fig. 7).

The crystal symmetry for each of these lattices is defined by the positions and identities of the inorganic cores. This enables a strategy to increase the complexity of lattices that can be synthesized by using "hollow" (or coreless) particles and therefore the sixth rule is:

The crystal symmetry of a lattice is dictated by the position of the inorganic cores; an SNA with no inorganic core can be used to "delete" a particle at a specified position within a unit cell.

These particles without inorganic cores are achieved by first functionalizing a gold particle with DNA, then cross-linking the DNA strands at the particle surface [29]. The gold particle can then be dissolved and, because the DNA strands are covalently attached to one another, the SNA retains its overall structure and binding properties [41]. When these SNAs with no inorganic core are used to assemble superlattices, they act as placeholders in the assembly process – they occupy a specific site within a unit cell and stabilize the lattice, but do not actually contribute to the arrangement of particles that defined the crystal symmetry. As an example, if one uses a hollow particle in place of one of the SNA-NPs in a bcc lattice, the bcc lattice becomes a simple cubic arrangement (Fig. 8). When using an AlB_2-type structure as a template, this strategy enables the synthesis of either simple hexagonal or graphite-like lattices when the hollow particle has the smaller or larger hydrodynamic radius, respectively (Fig. 8).

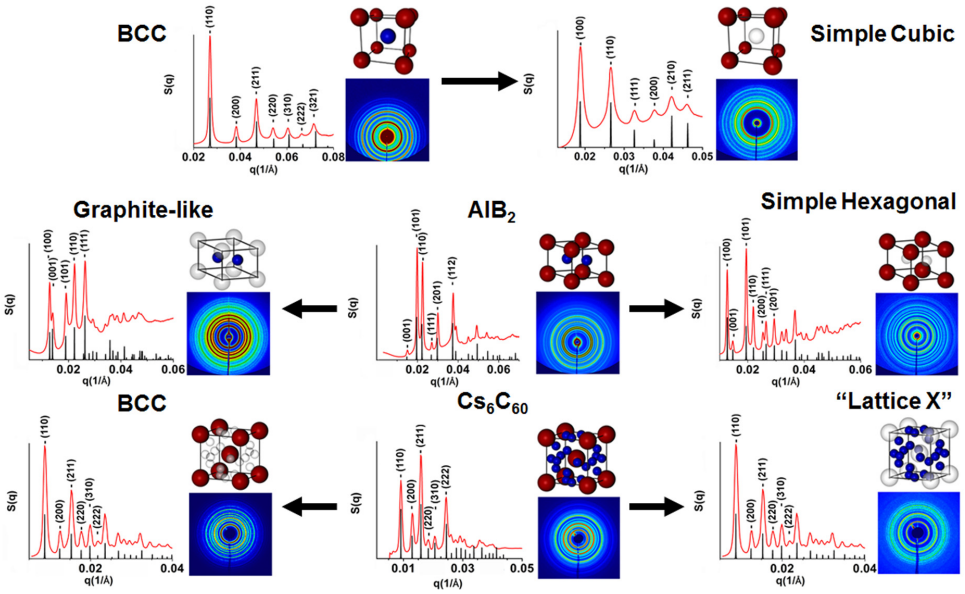

Figure 8. Utilizing a SNA with no inorganic core enables one to synthesize lattices where a particular nanoparticle type has been "deleted" from the unit cell. Note that the coreless SNAs are synthesized prior to superlattice formation, as opposed to being removed post-superlattice assembly. Figure adapted from ref. 41 (reprinted with permission from publisher).

If one assembles a Cs_6C_{60}-type lattice with hollow particles, it transforms to either a bcc lattice (when the smaller particle has a hollow core), or a lattice with no known mineral equivalent (when the larger particle has a hollow core). Because this lattice has not been constructed in any other method to date, it has no name and is therefore referred to as ''lattice X''. (Fig. 8) The construction of this symmetry highlights the complexity with which one can program crystallographic symmetry using DNA and nanoparticles as building blocks.

Each of the superlattices discussed so far have utilized spherical particles as building blocks, which limits them to inherently isotropic interactions with adjacent particles. However, if one utilizes particles of different shapes, these different geometries can be used to direct DNA interactions between particles along specific vectors [42]. This is because DNA hybridization will be maximized with particles align themselves to have their largest facets facing one another.

The seventh rule in DNA-directed particle assembly is thus:

Nanoparticle superlattices based upon anisotropic particles with flat faces will assemble into a lattice that maximizes the amount of parallel, face-to-face interactions between particles.

When DNA strands are attached to a planar surface, they all tend to point in the same direction in order to minimize repulsive interactions between adjacent strands, and thus the sticky ends are all positioned at a specific distance away from the particle surface. This means that, when two particles with flat faces approach one another, a significantly larger number of DNA connections will be made when those two particles are aligned with their flat faces parallel to one another, as this will position all of the DNA strands on those faces such that they can engage in hybridization. There is therefore a huge thermodynamic preferences for aligning anisotropic particles in this manner, and this can be used to dictate crystal symmetry [43]. When utilizing flat triangular prisms (thickness of ~7 nm, triangular edge length variable between 40 and 150 nm), which are essentially planar structures, a one-dimensional lamellar stack of prisms is obtained, where all of the prisms are aligned face to face (Fig. 9). Alternatively, rod-like structures arrange themselves in a hexagonal array, as this maximizes DNA interactions between the long axes of the rods (Fig. 9). Rhombic dodecahedra (a twelve-sided polyhedron that naturally packs into an fcc lattice) forms the predicted fcc structure, but importantly, each particle in the lattice has both positional and rotational ordering. This means that each particle within the lattice is aligned with their flat faces parallel to one another (Fig. 9). Similarly, octahedra (eight-sided polyhedral) adopt a bcc conformation with positional and rotational order, where each particle is surrounded by 8 nearest neighbors (Fig. 9).

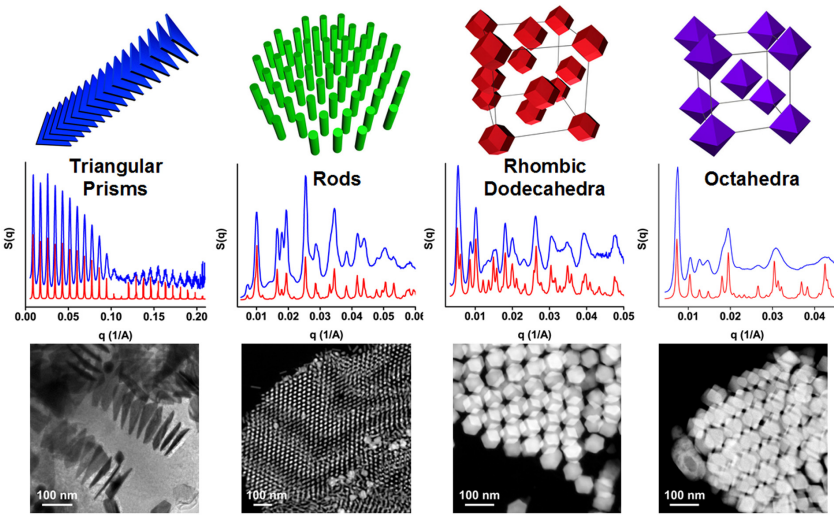

Figure 9. Anisotropic particles form superlattices that maximize the amount of parallel, face-to-face interactions between adjacent particles, as this maximizes the possibility for DNA hybridization events to occur. Figure adapted from ref. 42 (reprinted with permission from publisher).

Conclusions

In this work, a series of design rules has been presented that enable one to utilize programmable DNA interactions to generate a large number of nanoparticle superlattices. These rules provide access to a readily manipulated design space, where factors such as crystallographic symmetry, lattice parameters, and particle sizes can be independently controlled. This enables the synthesis of a wide variety of crystal structures that cannot be generated through other assembly techniques. These superlattices can be synthesized from particles of over an order of magnitude of different sizes, and the lattice parameters can be tuned over a few hundred nanometers. Importantly, these rules allow one to independently control factors such as interparticle distance, crystal symmetry, and particle identity. Because these factors can be used to influence the emergent properties of nanoparticle superlattices, this methodology should prove useful in generating designer materials with programmable physical properties.

Future directions will include the synthesis of nanoparticles of different material compositions, as well as the experimental investigation of unique plasmonic, photonic, magnetic, or catalytic properties of these unique structures [4, 12, 22, 44 – 46].

References

[1] Pauling, L. (1960) The nature of the chemical bond and the structure of molecules and crystals; an introduction to modern structural chemistry, 3rd ed., Cornell University Press, Ithaca, N.Y.

[2] Brus, L.E. (1983) *Journal of Chemical Physics* **79**:5566 – 5571. http://dx.doi.org/10.1063/1.445676.

[3] Burda, C., Chen, X.B., Narayanan, R., El-Sayed, M.A. (2005) *Chemical Reviews* **105**:1025 – 1102. http://dx.doi.org/10.1021/cr030063a.

[4] Daniel, M.C., Astruc, D. (2004) *Chemical Reviews* **104**:293 – 346. http://dx.doi.org/10.1021/cr030698+.

[5] Kelly, K.L., Coronado, E., Zhao, L.L., Schatz, G.C. (2003) *Journal of Physical Chemistry B* **107**:668 – 677. http://dx.doi.org/10.1021/jp026731y.

[6] Link, S., El-Sayed, M.A. (1999) *Journal of Physical Chemistry B* **103**:8410 – 8426. http://dx.doi.org/10.1021/jp9917648.

[7] Rossetti, R., Nakahara, S., Brus, L.E. (1983) *Journal of Chemical Physics* **79**:1086 – 1088. http://dx.doi.org/10.1063/1.445834.

[8] Xia, Y.N., Yang, P.D., Sun, Y.G., Wu, Y.Y., Mayers, B., Gates, B., Yin, Y.D., Kim, F., Yan, Y.Q. (2003) *Advanced Materials* **15**:353 – 389. http://dx.doi.org/10.1002/adma.200390087.

[9] Ajayan, P.M. (1999) *Chemical Reviews* **99**:1787 – 1799. http://dx.doi.org/10.1021/cr970102g.

[10] Alivisatos, A.P. (1996) *Science* **271**:933 – 937. http://dx.doi.org/10.1126/science.271.5251.933.

[11] Fernandez-Garcia, M., Martinez-Arias, A., Hanson, J.C., Rodriguez, J.A. (2004) *Chemical Reviews* **104**:4063 – 4104. http://dx.doi.org/10.1021/cr030032f.

[12] Law, M., Goldberger, J., Yang, P.D. (2004) *Annual Review of Materials Research* **34**:83 – 122. http://dx.doi.org/10.1146/annurev.matsci.34.040203.112300.

[13] Oh, M., Mirkin, C.A. (2005) *Nature* **438**:651 – 654. http://dx.doi.org/10.1038/nature04191.

[14] Spokoyny, A.M., Kim, D., Sumrein, A., Mirkin, C.A. (2009) *Chemical Society Reviews* **38**:1218 – 1227.
http://dx.doi.org/10.1039/b807085g.

[15] Trindade, T., O'Brien, P., Pickett, N.L. (2001) *Chemistry of Materials* **13**:3843 – 3858.
http://dx.doi.org/10.1021/cm000843p.

[16] Xia, Y.N., Xiong, Y.J., Lim, B., Skrabalak, S.E. (2009) *Angewandte Chemie – International Edition* **48**:60 – 103.
http://dx.doi.org/10.1002/anie.200802248.

[17] Macfarlane, R.J., Lee, B., Jones, M.R., Harris, N., Schatz, G.C., Mirkin, C.A. (2011) *Science* **334**:204 – 208.
http://dx.doi.org/10.1126/science.1210493.

[18] Mirkin, C.A., Letsinger, R.L., Mucic, R.C., Storhoff, J.J. (1996) *Nature* **382**:607 – 609.
http://dx.doi.org/10.1038/382607a0.

[19] Mucic, R.C., Storhoff, J.J., Mirkin, C.A., Letsinger, R.L. (1998) *Journal of the American Chemical Society* **120**:12674 – 12675.
http://dx.doi.org/10.1021/ja982721s.

[20] Kalsin, A.M., Fialkowski, M., Paszewski, M., Smoukov, S.K., Bishop, K.J.M, Grzybowski, B.A. (2006) *Science* **312**:420 – 424.
http://dx.doi.org/10.1126/science.1125124.

[21] Shevchenko, E.V., Talapin, D.V., Kotov, N.A., O'Brien, S., Murray, C.B. (2006) *Nature* **439**:55 – 59.
http://dx.doi.org/10.1038/nature04414.

[22] Talapin, D.V., Lee, J.S., Kovalenko, M.V., Shevchenko, E.V. (2010) *Chemical Reviews* **110**:389 – 458.
http://dx.doi.org/10.1021/cr900137k.

[23] Cutler, J.I., Zheng, D., Xu, X.Y., Giljohann, D.A., Mirkin, C.A. (2010) *Nano Letters* **10**:1477 – 1480.
http://dx.doi.org/10.1021/nl100477m.

[24] Hurst, S.J., Lytton-Jean, A.K.R., Mirkin, C.A. (2006) *Analytical Chemistry* **78**:8313 – 8318.
http://dx.doi.org/10.1021/ac0613582.

[25] Lee, J.S., Lytton-Jean, A.K.R., Hurst, S.J., Mirkin, C.A. (2007) *Nano Letters* **7**:2112 – 2115.
http://dx.doi.org/10.1021/nl071108g.

[26] Xue, C., Chen, X., Hurst, S.J., Mirkin, C.A. (2007) *Advanced Materials* **19**:4071 – 4074.
http://dx.doi.org/10.1002/adma.200701506.

[27] Young, K.L., Scott, A.W., Hao, L.L., Mirkin, S.E., Liu, G.L., Mirkin, C.A. (2012) *Nano Letters* **12**:3867 – 3871.
http://dx.doi.org/10.1021/nl3020846.

[28] Mitchell, G.P., Mirkin, C.A., Letsinger, R.L. (1999) *Journal of the American Chemical Society* **121**:8122 – 8123.
http://dx.doi.org/10.1021/ja991662v.

[29] Cutler, J.I., Zhang, K., Zheng, D., Auyeung, E., Prigodich, A.E., Mirkin, C.A. (2011) *Journal of the American Chemical Society* **133**:9254 – 9257.
http://dx.doi.org/10.1021/ja203375n.

[30] Lytton-Jean, A.K.R., Mirkin, C.A. (2005) *Journal of the American Chemical Society* **127**:12754 – 12755.
http://dx.doi.org/10.1021/ja052255o.

[31] Rosi, N.L., Giljohann, D.A., Thaxton, C.S., Lytton-Jean, A.K.R., Han, M.S., Mirkin, C.A. (2006) *Science* **312**:1027 – 1030.
http://dx.doi.org/10.1126/science.1125559.

[32] Elghanian, R., Storhoff, J.J., Mucic, R.C., Letsinger, R.L., Mirkin, C.A. (1997) *Science* **277**:1078 – 1081.
http://dx.doi.org/10.1126/science.277.5329.1078.

[33] Thaxton, C.S., Elghanian, R., Thomas, A.D., Stoeva, S.I., Lee, J.S., Smith, N.D., Schaeffer, A.J., Klocker, H., Horninger, W., Bartsch, G., Mirkin, C.A. (2009) *Proceedings of the National Academy of Sciences of the U.S.A.* **106**:18437 – 18442.
http://dx.doi.org/10.1073/pnas.0904719106.

[34] Giljohann, D.A., Seferos, D.S., Prigodich, A.E., Patel, P.C., Mirkin, C.A. (2009) *Journal of the American Chemical Society* **131**:2072 – 2073.
http://dx.doi.org/10.1021/ja808719p.

[35] Park, S.J., Lazarides, A.A., Storhoff, J.J., Pesce, L., Mirkin, C.A. (2004) *Journal of Physical Chemistry B* **108**:12375 – 12380.
http://dx.doi.org/10.1021/jp040242b.

[36] Park, S.Y., Lytton-Jean, A.K.R., Lee, B., Weigand, S., Schatz, G.C., Mirkin, C.A. (2008) *Nature* **451**:553 – 556.
http://dx.doi.org/10.1038/nature06508.

[37] Hill, H.D., Macfarlane, R.J., Senesi, A.J., Lee, B., Park, S.Y., Mirkin, C.A. (2008) *Nano Letters* **8**:2341 – 2344. http://dx.doi.org/10.1021/nl8011787.

[38] Macfarlane, R.J., Jones, M.R., Senesi, A.J., Young, K.L., Lee, B., Wu, J.S., Mirkin, C.A. (2010) *Angewandte Chemie – International Edition* **49**:4589 – 4592. http://dx.doi.org/10.1002/anie.201000633.

[39] Macfarlane, R.J., Lee, B., Hill, H.D., Senesi, A.J., Seifert, S., Mirkin, C.A. (2009) *Proceedings of the National Academy of Sciences of the U.S.A.* **106**:10493 – 10498. http://dx.doi.org/10.1073/pnas.0900630106.

[40] Woodcock, L.V. (1997) *Nature* **385**:141 – 143. http://dx.doi.org/10.1038/385141a0.

[41] Auyeung, E., Cutler, J.I., Macfarlane, R.J., Jones, M.R., Wu, J.S., Liu, G., Zhang, K., Osberg, K.D., Mirkin, C.A. (2012) *Nature Nanotechnology* **7**:24 – 28. http://dx.doi.org/10.1038/nnano.2011.222.

[42] Jones, M.R., Macfarlane, R.J., Lee, B., Zhang, J.A., Young, K.L., Senesi, A.J., Mirkin, C.A. (2010) *Nature Materials* **9**:913 – 917. http://dx.doi.org/10.1038/nmat2870.

[43] Jones, M.R., Macfarlane, R.J., Prigodich, A.E., Patel, P.C., Mirkin, C.A. (2011) *Journal of the American Chemical Society* **133**:18865 – 18869. http://dx.doi.org/10.1021/ja206777k.

[44] Bell, A.T. (2003) *Science* **299**:1688 – 1691. http://dx.doi.org/10.1126/science.1083671.

[45] Halas, N.J., Lal, S., Chang, W.S., Link, S., Nordlander, P. (2011) *Chemical Reviews* **111**:3913 – 3961. http://dx.doi.org/10.1021/cr200061k.

[46] Jones, M.R., Osberg, K.D., Macfarlane, R.J., Langille, M.R., Mirkin, C.A. (2011) *Chemical Reviews* **111**:3736 – 3827. http://dx.doi.org/10.1021/cr1004452.